Soft Inductive Tactile Sensor Using Flow-Channel Enclosing Liquid Metal

Shota Hamaguchi, Takumi Kawasetsu, Takato Horii, Hisashi Ishihara, Ryuma Niiyama, Koh Hosoda, and Minoru Asada

***Abstract*—There are structural challenges in increasing the softness of conventional soft tactile sensors because rigid electrical elements have to be installed around the sensing areas, which should be compressive, stretchable, and durable. To solve these issues, we propose an inductive tactile sensor whose silicone-rubber body has only two liquid-metal reservoirs connected by an elongated flow channel. When one reservoir is placed around the sensing area, another one can be placed at a non-sensing area. Furthermore, in this structure, touch can be detected by monitoring the inflow and outflow of the liquid-metal in the latter reservoir by using a separately placed coil circuit based on the eddy-current effect. The proposed method requires no direct electrical connections with liquid metal in the reservoirs or flow channels. This means that the sensor body has no inhibitor that reduces its compressibility and stretchability, and that deteriorates its durability. The experimental results demonstrated that larger reservoir diameters provided larger sensitivity and higher signal-to-noise ratio of approximately 65 dB. Additionally, we observed that the bending of the body does not affect the sensor response as much as gravity. Therefore, we conclude that our sensor has structural advantages for tactile-sensor installation, especially in soft actuators, because our completely soft sensor does not experience reduction or deterioration in its functionality owing to its softness.**

Manuscript received October 15, 2019; accepted March 4, 2020. Date of publication April 6, 2020; date of current version April 24, 2020. This letter was recommended for publication by Associate Editor Dr. C. Majidi and Editor C. Laschi upon evaluation of the reviewers' comments. This work was supported in part by a project (Project for Innovative AI Chips and Next-Generation Computing Technology Development/(2) Development of next-generation computing technologies/ Exploration of Neuromorphic Dynamics towards Future Symbiotic Society) commissioned by the New Energy and Industrial Technology Development Organization (NEDO), in part by PRESTO, JST under Grant JPMJPR1652, and in part by JSPS KAKENHI Grant-in-Aid for Scientific Research on Innovative Areas "Science of Soft Robot" project under Grant JP18H05466. *(Corresponding author: Takumi Kawasetsu.)*

Shota Hamaguchi is with the Faculty of Engineering, Mie University, 5148507 Tsu, Japan (e-mail: 417191@m.mie-u.ac.jp).

Takumi Kawasetsu and Ryuma Niiyama are with the Graduate School of Information Science and Technology, The University of Tokyo, Tokyo 1138656, Japan (e-mail: kawasetsu@isi.imi.i.u-tokyo.ac.jp; niiyama@isi.imi.i.u-tokyo.ac.jp).

Takato Horii and Koh Hosoda are with the Graduate School of Engineering Science, Osaka University, Osaka 5650871, Japan (e-mail: takato@sys.es.osaka-u.ac.jp; hosoda@sys.es.osaka-u.ac.jp).

Hisashi Ishihara is with the Graduate School of Engineering, Osaka University, Osaka 5650871, Japan, with the JST PRESTO, Tokyo 102-0076, Japan, and also with the Institute for Open and Transdisciplinary Research Initiatives, Osaka University, Osaka 5650871, Japan (e-mail: ishihara@ams.eng.osaka-u.ac.jp).

Minoru Asada is with the Institute for Open and Transdisciplinary Research Initiatives, Osaka University, Osaka 5650871, Japan (e-mail: asada@otri.osaka-u.ac.jp).

This article has supplementary downloadable material available at http://ieeexplore.ieee.org, provided by the authors.

Digital Object Identifier 10.1109/LRA.2020.2985573

***Index Terms*—Soft sensors and actuators, force and tactile sensing.**

I. Introduction

THE soft structure in a soft robot [1]–[4] makes rich contact with physical environment, allowing completely effective and safe interactions to be achieved. The use of open-loop control has been sufficient for demonstrating basic tasks; however, finer movements and environmental changes require sensors for feedback control. Sensors required for soft robots include tactile sensors, which obtain information from physical interactions with the environment, i.e., a deformation of soft materials and the contact information.

Many studies proposed several types of soft tactile sensors [5], [6] and tried to install them to soft pneumatic actuators, e.g., [7]-[9]. However, ignorable technical issues have arisen when embedding or adhering tactile sensor elements in a soft-material sensor body. As discussed in [10], the following issues need to be solved: 1) embedding fragile sensor elements, e.g., electric elements and wires, into soft materials deteriorates the sensor durability; 2) embedding rigid materials into soft materials reduces the softness of the sensor body; and 3) adhering rigid sensor elements with soft materials introduces an unavoidable stress concentration and a weak interface.

One of the promising approaches used to solve these issues is the application of a soft inductive tactile sensor. Kawasetsu *et al.* [11] proposed an inductive tactile sensor by employing a liquid-metal reservoir in a silicone-rubber body as a positional marker and a coil directly below the contact area as a position detector of the liquid metal. The proposed sensor enables the removal of both fragile electrical elements and hard materials from silicone rubber, as well as electrical connections with the liquid metal. By contrast, the previously developed inductive tactile sensors require placing a coil circuit directly below the contact area, thereby reducing the softness of the sensor. This limitation becomes an issue to be addressed when installing an inductive tactile sensor into entirely soft robots, e.g., soft pneumatic actuators [7]-[9]. Structural improvements are required to remove the coil circuit from the contact area and to realize a totally soft tactile sensor with a liquid-metal reservoir, which is suitable for implementation in such soft actuators.

Therefore, we propose a soft inductive tactile sensor made of a coil circuit and a silicone rubber, with a long liquid-metal-flow channel connected to two reservoirs [see Fig. 1]. Employing an inductive sensing technology and the liquid-metal-flow channel

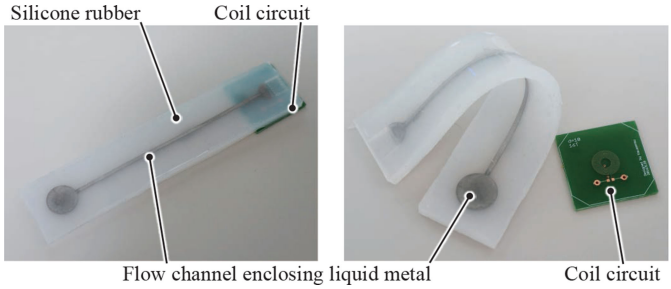

Fig. 1. Appearance of the proposed inductive tactile sensor. The sensor consists of a coil circuit and silicone rubber with a long liquid-metal-flow channel connected to two reservoirs. The sensor can estimate the applied normal force by measuring the displacement of the liquid metal in the flow channel as the change in inductance of the coil.

enables to place the coil circuit near one of the reservoirs that is far from the contact area, as well as remove the direct electrical connections with the silicone rubber or the liquid metal. We examined that the sensor could measure the applied normal force with sufficient accuracy by measuring the inductance of the coil. The results demonstrated that the sensitivity of the sensor increased upon increasing the diameter of the disk-shaped reservoir where force was applied. We also examined the sensor sensitivity against bending and, subsequently, confirmed that the sensor response did not exhibit a clear correlation with the bending. On the basis of these results, we discuss the method for determining the structural-design parameters of the sensor, and we summarize the practical issues to be addressed in the future.

II. Related Works

This section summarizes the previously developed soft tactile sensors [5], [6]. We also discuss the remaining issues of these conventional sensors.

One of the simple methods to fabricate a soft tactile sensor is to implement electrical elements, such as a strain gauge, into flexible materials [12]. Upon applying a contact force to the soft material containing a strain gauge, the gauge is deformed, and, accordingly, the resistance of the gauge also changes. Consequently, we can estimate the applied contact force by measuring the change in resistance of the gauge. While the fabrication process and working principle of this kind of sensor is simple, the following issues still exist: 1) a reduction in the softness and stretchability of the soft material owing to the embedding of the hard electrical elements; 2) low durability of the embedded fragile electrical elements; and 3) ease of detachment of different embedded electrical elements from soft materials owing to different softness and stretchability. These issues mainly arise from the differences in softness and stretchability between the soft materials and embedded electrical elements. With the recent growth in material engineering, stretchable electrical elements and wires have been proposed; however, their softness, stretchability, and durability against repeated loads are still not sufficient compared with soft sensor body materials such as silicone rubber.

Several studies proposed soft tactile sensors that measure the electrical resistance of a micro-fluid channel embedded in a soft-material soft sensor body. Mainly, the micro-fluid channel is filled with liquid metal [8], [13] or ionic gel [9], [14]-[16]. Upon applying a contact force to the sensor body, the cross-sectional area of the channel decreases, and, consequently, the electrical resistance of the filled liquid metal or of the ionic gel increases. Thus, we can estimate the applied force by measuring the resistance change of the channel by using electrodes. This type of sensor is highly soft and stretchable because the sensor body contains only micro-fluid channels. The remaining issue is that the sensor requires to insert electrodes or wires into the channel to measure the resistance. As discussed previously, the adhesion between metal wires and soft materials with different values of softness and stretchability causes deterioration in the durability of the sensor.

Soft tactile sensors based on an electromagnetic phenomenon can be used to remove electrical elements from a soft material. Magnetic tactile sensors, which consist of a magnet embedded in a soft material and a magnetic sensor placed outside the soft material, measure the applied force based on the change in magnetic field [17]-[19]. As another type of tactile sensor employing an electromagnetic phenomenon, inductive tactile sensors, which measure the change in electromagnetic field around sensor bodies with coils, have been proposed [10], [11], [20]-[24]. In this structure, some metallic ingredients, such as iron particles [10], [20], [21], [24] and liquid metal [11], are locally placed in a soft material, and a coil circuit is mounted around these ingredients outside the soft material. Upon applying a contact force to the soft material, the iron particles or liquid metal displaces in the material, following which the positional relationship between the coil and them changes. The inductance of the coil changes because of the spatial-permeability changes or the eddy-current effect, and, as a result, we can estimate the contact force on the basis of the change in inductance. Inductive sensing enables to fabricate a highly soft and stretchable tactile sensor with high durability because its soft materials do not contain any fragile electrical elements. However, the sensor requires to install a coil circuit at a close distance from the iron particles or liquid metal.

As a similar method, vision-based tactile sensors, which monitor the deformation of soft materials by using optical sensors, were proposed. Soft tactile sensors employing an optical waveguide and a combination of an LED and a photodiode were also proposed [25], [26]. One of the remaining issues regarding these sensors is to distinguish the sensor response caused by bending or applied contact force. Soter *et al.* [27] proposed a method for measuring the displacement of a colored liquid filled in transparent tubes, using an external camera. This kind of sensor is also one of the promising methods to measure the contact forces applied to soft materials without embedding any electrical elements, when the sensor has sufficient space for camera imaging.

To address these issues, the proposed sensor employs an inductive sensing technique with a flow channel enclosing liquid metal. This structure realizes a high softness, stretchability, and durability owing to 1) a lack of hard materials within the soft materials and near the contact area, 2) no direct electrical connections to the liquid metal or the flow channel.

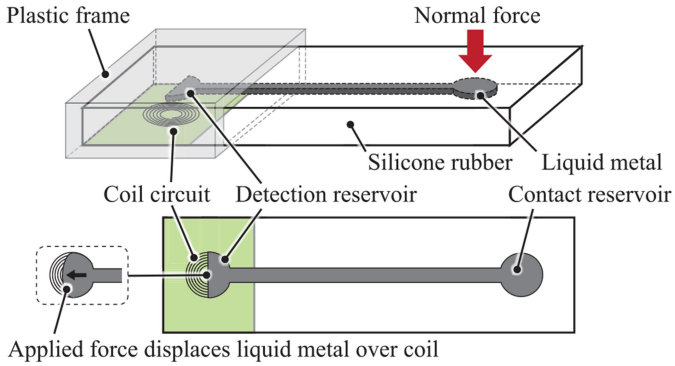

Fig. 2. Structure and working principle of the proposed tactile sensor that can estimate the applied normal force by measuring the inductance change of a coil. Upon applying a normal force onto the contact reservoir, the liquid metal moves toward the detection reservoir via the flow channel. As a result, the detection reservoir expands toward left (lower figure), causing inductance change.

III. Inductive Tactile Sensor With Liquid-Metal-Flow Channel

A. Working Principle

Fig. 2 depicts the structure and working principle of the proposed tactile sensor. The sensor comprises a rectangular sensor body made of silicone rubber, liquid metal, and a coil printed on a circuit board. Furthermore, the sensor body has a flow channel for enclosing the liquid metal. This flow channel consists of a disk-shaped reservoir (hereafter referred to as contact reservoir), a half-disk-shaped reservoir (hereafter referred to as detection reservoir), and a linear channel that connects them. The detection reservoir has a thin silicone-rubber wall that separates the liquid metal from the outside of the rubber. A spiral coil has the same radius as that of the detection reservoir, and it is placed under the detection reservoir.

The proposed sensor can estimate the applied normal force by measuring the displacement of the liquid metal in the detection reservoir on the basis of the following mechanism: Upon applying a normal force onto the contact reservoir, the liquid metal in the reservoir is pushed out toward the detection reservoir via the linear channel. Consequently, the pushed-out liquid metal expands the detection reservoir by pushing out the thin wall. Because the thickness of the wall can be deformed more easily than other parts of the sensor body, the expansion direction is limited to the left direction, as depicted in the bottom of Fig. 2. Therefore, the amount of liquid metal over the coil is increased according to the applied force. Here, the coils can be utilized as a metal detector by using an eddy-current effect, meaning that inductance of the coils changes according to the position of conductors near the coils. Increasing the amount of the liquid metal over the coil in the proposed sensor increases the eddy current in the liquid metal, consequently decreasing the coil inductance. Thus, we can estimate the applied normal force by monitoring the change in the coil inductance.

B. Fabrication Process

Fig. 3(a)–(c) illustrates the fabrication process of the silicone-rubber sensor body holding a flow channel filled with liquid metal. First, a silicone sheet with a groove of a flow channel was fabricated by pouring uncured silicone rubber into a three-dimensional (3D) printed female mold [see Fig. 3(a)]. In this study, we employed a platinum-cured silicone rubber (Ecoflex 00-30, Smooth-On Inc., USA). After curing the rubber sheet, it was set in another 3D-printed female mold. Then, liquid metal was poured into the flow channel in the rubber sheet [see Fig. 3(b)]. We here employed eutectic galliumindium (eGaIn [28]; 75 wt.%. Ga and 25 wt.% In) with the melting point of 15.5 °C as the liquid metal. Finally, uncured silicone rubber was poured on the rubber sheet to form the cover enclosing the liquid metal (Fig. 3(c)). Here, a plastic rectangular small block was placed beside the detection reservoir to provide the space where the detection reservoir could easily expand in the left direction

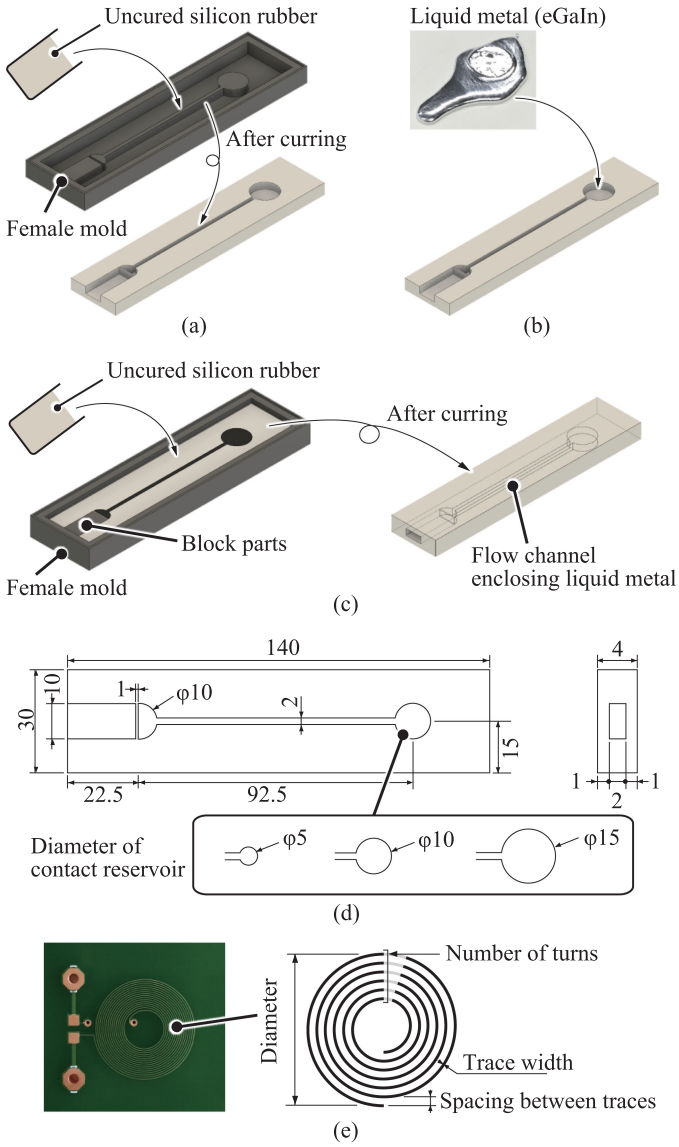

Fig. 3. Fabrication process and design parameters of the proposed sensor: (a) pouring uncured silicone rubber into the female mold to fabricate the flow channel; (b) pouring liquid metal into the flow channel; (c) enclosing the liquid metal by pouring the uncured silicone rubber; (d) design parameters of a silicone rubber holding a flow channel; (e) design parameters of a dual-layer spiral coil for detecting the displacement of liquid metal.

[see Fig. 2 bottom] with the sensor body. After the rubber cured, the block was removed from the rubber sheet.

Fig. 3(d) summarizes the design parameters of the fabricated silicone-rubber sheet holding a flow channel. In this study, we fabricated nine types of sensor bodies to investigate the relationship between the design parameters and sensor-response properties. These sensor bodies were different in the combination of the contact-reservoir diameter and the channel thickness. The contact-reservoir diameter was selected from 5, 10, and 15 mm, and the channel thickness from 1, 2, and 3 mm. For the nine types of sensor bodies, other structural parameters were common: The detection-reservoir diameter was 10 mm, which is the same as that of the coil diameter. The detection-reservoir-wall thickness was 1 mm. The linear-channel width was 2 mm and the linear-channel length 92.5 mm between the centers of both the reservoirs. The long-side and short-side lengths of the sensor body were 140 and 30 mm, respectively. The sensor-body thicknesses above and below the channel were 1 mm. Therefore, the total thickness of the sensor was the summation of these thicknesses (2 mm) and that of the channel; e.g., the total thickness of the sensor with 3-mm channel was 5 mm.

We fabricated a dual-layer planar spiral coil installed on a printed circuit board to detect the liquid-metal displacement by employing a PCB manufacturing service (P-ban.com Corp., Japan). As depicted in Fig. 3(e), the coil diameter was 10 mm, and the number of turns was 16 in one layer. The width of the trace and the interval between the traces were both 0.1 mm. A 330-pF ceramic capacitor was connected in parallel to the coil to employ an inductance-to-digital converter [29].

IV. Experiments

A. Method

We investigated the relationship between the inductance changes and the applied normal force or bending by using the setup depicted in Fig. 4. The sensor was mounted on a tri-axis robot stage (TTA-C3-WA-30-25-10, IAI Corp., Japan) holding a plastic cylindrical indenter with a diameter of 20 mm. A forcetorque sensor (F/T sensor; Mini 2/10-A, BL Autotech Ltd., Japan) was inserted between the tri-axis stage and the indenter to measure the normal forces applied to the sensor. Both the inductance and the output of the F/T sensor were obtained using the inductance-to-digital converter (LDC1614, Texas Instruments Inc., USA) and an analog-to-digital converter (AI-1664LAX-USB, CONTEC Corp, Japan), respectively. The sampling period was set to 20 ms. As stated in Section III, we prepared nine types of sensor bodies, all of which had three different contact-reservoir diameters (5, 10, and 15 mm) and three different flow-channel thicknesses (1, 2, and 3 mm). The sensor was pushed using the indenter at a contact speed of 0.1 mm/s until the applied normal force reached 25 N. This measurement was repeated 10 times for each sensor body.

As depicted in Fig. 4(b), a 3D-printed curved block was placed under the rubber of the sensor to measure the inductance change against the bending. We prepared six blocks with six different curvatures as follows: R300, 250, 200, 150, 100, and 75.

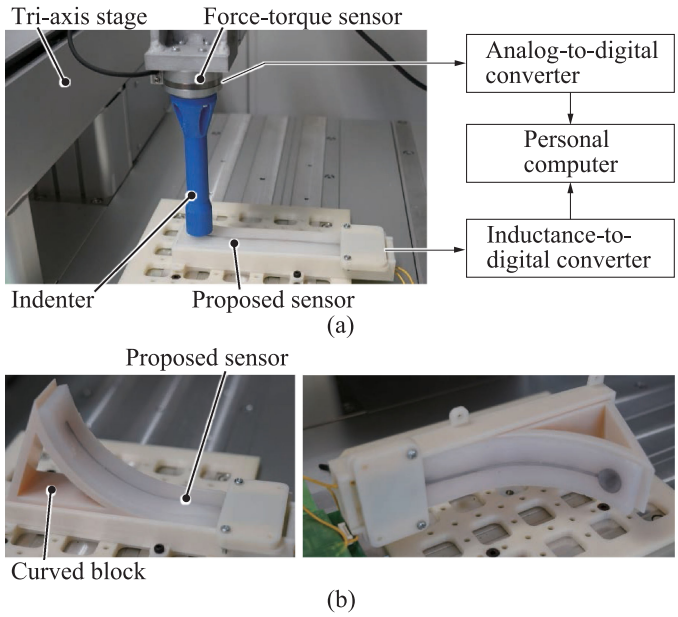

Fig. 4. Experimental setup: (a) measurement of the relationship between inductance change and applied normal force; (b) measurement of the relationship between inductance change and bending applied in the vertically upward direction (left) or horizontal direction (right).

B. Results

1) Inductance Change Versus Applied Normal Force: Fig. 5 depicts the inductance change versus the applied normal force for the nine types of prepared sensor bodies, all of which have different contact-reservoir diameters and different flow-channel thicknesses. In each plot, the horizontal axis denotes the applied normal force measured using the F/T sensor, while the vertical axis denotes the change in the inductance from its initial value, i.e., the inductance value at which no load was applied. The solid line indicates the mean inductance change of the 10 trials, and the shaded gray region indicates twice the standard deviation 2σ. The results demonstrate that the inductance decreases according to the normal force applied, and that the small shaded region compared with the response range shows a high repeatability of the changes in inductance. We also confirmed that the change in inductance tends to saturate upon applying a certain amount of normal force. In addition, a larger diameter of the contact reservoir causes a larger change in inductance irrespective of the thickness of the flow channel.

Subsequently, the sensitivities to the applied normal force were calculated and compared for the nine types of sensor bodies. We defined the initial sensitivity as the inductance change upon applying up to 5 N normal force from the initial inductance, and then the initial sensitivities of the nine types of sensor bodies were calculated. Fig. 5(d) depict a part of the plot of Fig. 5(b) in the range of the applied normal force up to 5 N. We employed linear approximation to these plots, following which the initial sensitivity was calculated using the slope of the linear-approximation graph. Fig. 5(e) indicates the calculated initial sensitivities for the nine types of sensor bodies. The horizontal axis denotes the contact-reservoir diameter, while the vertical axis denotes the initial sensitivity (μH/N). The

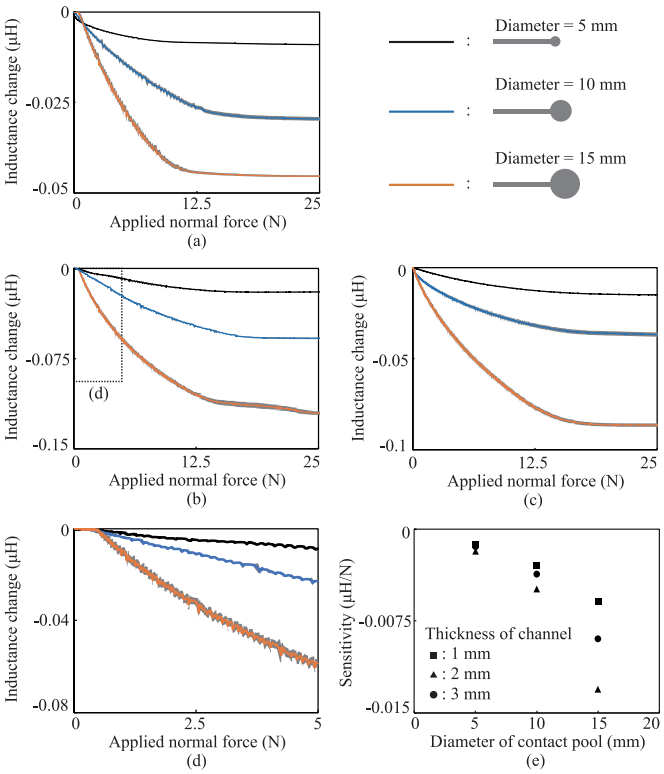

Fig. 5. Inductance change versus applied normal force for nine types of sensor bodies: (a), (b), and (c) depict the inductance change with the flow-channel thicknesses of 1, 2, and 3 mm, respectively; (d) depict a part of the plot of (b) in the range of the applied normal force up to 5 N; (e) the initial sensitivities obtained from linear-approximation result for each sensor body.

TABLE I
CALCULATED SNRS

Signal-to-noise ratio (dB)		Diameter of contact reservoir (mm)		
		5	10	15
Thickness of channel (mm)	1	42.10	52.54	58.50
	2	50.95	60.19	64.87
	3	46.33	59.47	61.60

square, triangular, and circular dots indicate the results for the flow-channel thicknesses of 1, 2, and 3 mm, respectively. The initial sensitivity increased quadratically upon increasing the contact-reservoir diameter.

We also evaluated the signal-to-noise ratio (SNR) for each sensor body. The SNR was calculated as follows: $20\log_{10}(A_S/A_N)$, where A_S denotes the maximum inductance change depicted in Fig. 5 and A_N the peak-to-peak inductance under the no-load condition. Table I presents the calculated SNRs. The results demonstrate that the SNR improved upon increasing the contact-reservoir diameter, and that large SNRs were obtained when the flow-channel thickness was 2 mm for the sensor bodies used in this study.

2) Inductance Change Versus Bending: We examined the sensor response to bending using three kinds of sensor bodies each having flow-channel thickness of 2 mm and contact-reservoir diameter of 5, 10, and 15 mm. Fig. 6 depicts the inductance change versus six different curvatures. The horizontal axis denotes the curvature (radius of the curved silicone

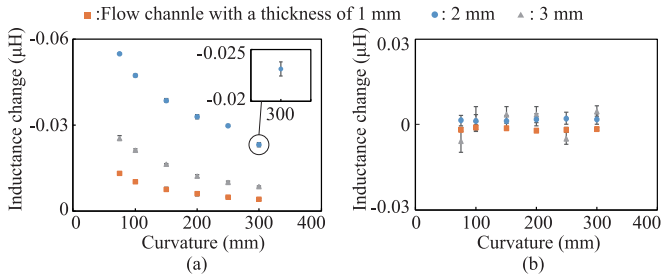

Fig. 6. Inductance change versus applied bending: (a) bending applied in the vertically upward direction, and (b) bending applied in the horizontal direction.

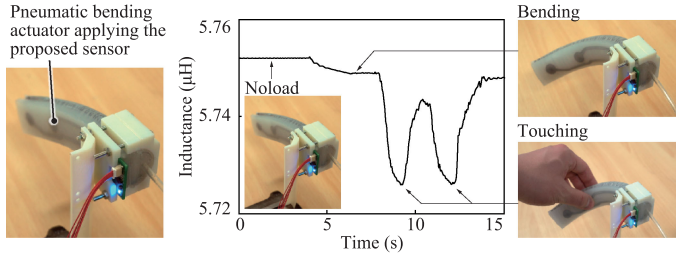

Fig. 7. Change in inductance versus bending and force applied to the proposed sensor attached to a pneumatic bending actuator.

rubber), while the vertical axis denotes the magnitude of the inductance change from the initial inductance value without bending. The square, circular, and triangular dots represent the contact-reservoir diameters of 5, 10, and 15 mm, respectively. Each dot denotes the mean inductance change across 10 trials, and the error bar is twice the standard deviation 2σ. First, the silicone rubbers were bent in the vertically upward direction [see Fig. 6(a)]. Subsequently, we confirmed that the inductance decreased quadratically upon decreasing the curvature, and that these inductance changes had a high repeatability. Next, the sensor body were bent in the horizontal direction [see Fig. 6(b)] to eliminate the effects of gravity from the sensor. The results demonstrate that the inductance changes were relatively small compared with the results where bending was applied in the vertically upward direction, and that the inductance changes did not exhibit a clear correlation with the bending.

As a demonstration of the possible applications of the proposed sensor, we attached the sensor to a pneumatic bending actuator [30]. Fig. 7 shows the changes in inductance of the proposed sensor under the corresponding state of the pneumatic actuator. We first applied bending to the actuator by increasing a pressure in the actuator, then touched the sensor to apply a force. The results indicate that the sensor responds to both the applied bending and force.

V. DISCUSSION

Our results indicate that the proposed sensor can estimate the normal force precisely even though it has the flow channel. First, Fig. 5 depicts that the widths of measurement variance (2σ) are quite small; in other words, the sensor can output approximately the same value against several touches. Additionally, the SNRs

are more than 40 dB for all the nine types of the sensor bodies prepared for this study, with highest SNR of approximately 65 dB. This means that our sensor can maintain high precision by investigating the relationship between the true input force and the sensor output, even if the structural parameters change.

Furthermore, the results presented in Section IV-A indicate that sensitivity and SNR are higher when the sensor has a larger reservoir, for any cross-sectional area of the flow channel. This tendency can be explained by the following mechanism: First, the coil inductance increases more when larger amount of liquid metal exists over the coil. Second, the amount of liquid metal over the coil increases more theoretically when the reservoir is larger, even when the indentation depth is the same. Thus, the sensor sensitivity can be increased by enlarging the size of the reservoir. However, the spatial resolution of the sensor decreases upon increasing the reservoir size.

Fig. 5(d) demonstrates that the proposed sensor does not respond at low force levels of approximately 0.2 N. This could be caused by an expansion of the flow channel itself before the liquid metal pushed out from the contact reservoir reaches the detection reservoir. Therefore, the minimal detectable force and the bending angle may depend on the shape and softness of the flow channel and the diameter of the reservoirs. The relationship between the minimal detectable force and the sensor structure should be investigated in a future work.

Although the sensitivity of the sensor was considered not to be affected by the cross-sectional area of the flow channel, yet it was considered to be affected only by the size of reservoir because the liquid metal was incompressible. The result demonstrates that the sensitivity was affected by the cross-sectional area of the flow channel: Fig. 5 indicates that the sensitivity was the highest in 2-mm thickness condition than those in 1- and 3-mm thickness ones. This can be explained by the following mechanisms: First, the pressure loss in the flow channel is larger in a thinner channel. Second, the expansion volume of the flow channel is larger in a thicker channel. Because of these two mechanisms, we have to determine the optimal flow-channel thickness that maximizes the sensor sensitivity. Both the aforementioned mechanisms will be investigated in detail in future studies.

Fig. 5 indicates that a sensor with a large contact reservoir has a large deviation, and that the responses have noise with the same frequency but with a different level. This could be from the slight vibrations generated by the moving indenter. A softer sensor body can generate larger vibrations of the body, resulting in larger vibrations of the liquid metal in the body. The sensor body softens upon increasing the diameter of the contact reservoir; thus, a large-diameter sensor shows a larger deviation than the others.

Regarding the effect of the sensor bending on the sensor response, the results in Fig. 6 suggest that the effect of bending is relatively small whereas that of gravity cannot be ignored. The effect of gravity on the changes in inductance can be explained as follows: when the location of the contact reservoir is higher than that of the detection reservoir, the liquid metal flows toward the detection reservoir in the flow channel, thereby decreasing the inductance. In addition, the change in inductance shows slightly larger deviations when the sensor was bent horizontally. This could be because the liquid metal moved within the flow channel owing to slight differences in height of the contact reservoir across the trials. Further investigations on the effect of gravity on the sensor response and a compensation method should be addressed in the future works.

When applying bending and normal forces simultaneously (Fig. 7), the isolation between these two responses may be difficult because the proposed sensor measures them as a movement of liquid metal in a flow channel. A sensor array holding a flow channel and coil pairs could be a possible approach to estimating the applied force and bending independently.

A distinctive characteristic of the sensor is that its body, along with the touch part and flow channel, is totally soft. This characteristic is advantageous for installing tactile sensors in soft actuators because the proposed sensor does not reduce the softness of the soft actuators. To realize totally soft actuators by using the proposed sensor, the possible fluctuations of the sensor output must be compensated according to the motion of the actuator. Therefore, such fluctuations should be investigated in the future works.

Because the sensor employs magnetic phenomena, the inductance may vary with electromagnetic interference, e.g., caused by an electric motor placed near a coil and another sensing coil applied as a sensor array. This is a common issue of magnetic or inductive tactile sensors; thus, this investigation and the use of a compensation method will be addressed in a future study.

VI. Conclusion

This study proposed a soft inductive tactile sensor that can estimate the applied normal force on the basis of the inductance change caused by the displacement of liquid metal enclosed in a flow channel. Employing an inductive sensing technology and a liquid-metal-flow channel enables the fabrication of a highly compressible, stretchable, and durable tactile sensor, without embedding any electrical elements in soft materials, and without any electrical connections with the soft materials. The proposed sensor has high accuracy and repeatability of its response, and its sensitivity increases upon increasing the diameter of the reservoir of the liquid metal where the contact force is applied. In addition, the results suggest that the effect of bending on sensor responses is relatively small compared to the response range.

The advantage of our highly compressible, stretchable, and durable sensor is its ease of installation on entirely soft robots, e.g., including soft pneumatic actuators. One of the future works is to realize the integration of our sensor and soft robots, e.g., a soft robotic hand composed of soft pneumatic actuators, to obtain rich information during physical interactions. We also try to miniaturize the sensor by fabricating fine flow channels to increase its spatial resolution.

Acknowledgment

The authors would like to thank Mr. Takumi Yamamoto for his assistance in preparing the experiments.

REFERENCES

[1] D. Rus and M. T. Tolley, "Design, fabrication and control of soft robots," *Nature*, vol. 521, pp. 467–475, 2015.

[2] S. Kim, C. Laschi, and B. Trimmer, "Soft robotics: A bioinspired evolution in robotics," *Trends Biotechnol.*, vol. 31, no. 5, pp. 287–294, 2013.

[3] J. Hughes, U. Culha, F. Giardina, F. Guenther, A. Rosendo, and F. Iida, "Soft Manipulators and Grippers: A Review," *Frontiers Robot. AI*, vol. 3, no. 69, pp. 1–12, 2016.

[4] C. Laschi, B. Mazzolai, and M. Cianchetti, "Soft robotics: Technologies and systems pushing the boundaries of robot abilities," *Sci. Robot.*, vol. 1, 2016, Art. no. eaah3690.

[5] R. S. Dahiya, G. Metta, M. Valle, and G. Sandini, "Tactile sensing—From humans to humanoids," *IEEE Trans. Robot.*, vol. 26, no. 1, pp. 1–20, Feb. 2010.

[6] H. Wang, M. Totaro, and L. Beccai, "Toward perceptive soft robots: Progress and challenges," *Adv. Sci.*, vol. 5, no. 9, 2018, Art. no. 1800541.

[7] K. Suzumori, S. Endo, T. Kanda, N. Kato, and H. Suzuki, "A bending pneumatic rubber actuator realizing soft-bodied Manta swimming robot," in *Proc. IEEE Int. Conf. Robot. Autom.*, 2007, pp. 4975–4980.

[8] Y. Hao, Z. Liu, Z. Xie, X. Fang, T. Wang, and L. Wen, "A variable degree-of-freedom and self-sensing soft bending actuator based on conductive liquid metal and thermoplastic polymer composites," in *Proc. IEEE/RSJ Int. Conf. Intell. Robot. Syst.*, 2018, pp. 8033–8038.

[9] R. L. Truby, R. K. Katzschmann, J. A. Lewis, and D. Rus, "Soft robotic fingers with embedded Ionogel sensors and discrete actuation modes for somatosensitive manipulation," in *Proc. IEEE Int. Conf. Soft Robot.*, 2019, pp. 322–329.

[10] T. Kawasetsu, T. Horii, H. Ishihara, and M. Asada, "Flexible tri-axis tactile sensor using spiral inductor and magnetorheological elastomer," *IEEE Sensors J.*, vol. 18, no. 14, pp. 5834–5841, Jul. 2018.

[11] T. Kawasetsu, R. Niiyama, and Y. Kuniyoshi, "Flexible and soft inductive tri-axis tactile sensor using liquid metal as sensing target," in *Proc. IEEE Sensors Conf.*, 2019, pp. 1–4.

[12] G. Gerboni, A. Diodato, C. Ciuti, M. Cianchetti, and A. Menciassi, "Feedback control of soft robot actuators via commercial flex bend sensors," *IEEE Trans. Mechatronics*, vol. 22, no. 4, pp. 1881–1888, Aug. 2017.

[13] T. Kim, S. J. Yoon, and Y. Park, "Soft inflatable sensing modules for safe and interactive robots," in *Proc. IEEE/RSJ Int. Conf. Intell. Robots Syst.*, 2018, pp. 3216–3223.

[14] J. Chossat, Y. Park, R. J. Wood, and V. Duchaine, "A soft strain sensor based on ionic and metal liquids," *IEEE Sensors J.*, vol. 13, no. 9, pp. 3405–3414, Sep. 2013.

[15] A. Fassler and C. Majidi, "Soft-matter capacitors and inductors for hyperelastic strain sensing and stretchable electronics," *Smart Mater. Struct.*, vol. 22, no. 5, Apr. 2013, Art. no. 055023.

[16] N. Lazarus, C. D. Meyer, S. S. Bedair, H. Nochetto and I. M. Kierzewski, "Multilayer liquid metal stretchable inductors," *Smart Mater. Struct.*, vol. 23, no. 8, Jul. 2013, Art. no. 085036.

[17] M. Goka, H. Nakamoto, and S. Takenawa, "A magnetic type tactile sensor by GMR elements and inductors," in *Proc. IEEE/RSJ Int. Conf. Intell. Robots Syst.*, 2010, pp. 885–890.

[18] L. Jamone, L. Natale, G. Metta, and G. Sandini, "Highly sensitive soft tactile sensors for an anthropomorphic robotic hand," *IEEE Sensors J.*, vol. 15, no. 8, pp. 4226–4233, Aug. 2015.

[19] T. P. Tomo *et al.*, "A new silicone structure for uSkin–A soft, distributed, digital 3-axis skin sensor and its integration on the humanoid robot iCub," *IEEE Robot. Autom. Lett.*, vol. 3, no. 3, pp. 2584–2591, Mar. 2018.

[20] T. Kawasetsu, T. Horii, H. Ishihara, and M. Asada, "Size dependency in sensor response of a flexible tactile sensor based on inductance measurement," in *Proc. IEEE Sensors Conf.*, 2017, pp. 1–3.

[21] O. Ozioko, M. hersh, and R. Dahiya, "Inductance-based flexible pressure sensor for assistive gloves," in *Proc. IEEE Sensors. Conf.*, 2018, pp. 1–4.

[22] D. Jones, J. W. Kow, A. Alazmani, and P. R. Culmer, "Computational design tools for soft inductive tactile sensors," in *Proc. 7th IEEE Int. Conf. Biomed. Robot. Biomechatronics*, 2018, pp. 871–876.

[23] H. Wang *et al.*, "Design and characterization of tri-axis soft inductive tactile sensors," *IEEE Sensors J.*, vol. 18, no. 19, pp. 7793–7801, Oct. 2018.

[24] H. Wang *et al.*, "A wireless inductive sensing technology for soft pneumatic actuators using magnetorheological elastomers," in *Proc. IEEE Int. Conf. Soft Robot.*, 2019, pp. 242–248.

[25] H. Zhao, K. O'Brien, S. Li, and R. F. Shepherd, "Optoelectronically innervated soft prosthetic hand via stretchable optical waveguides," *Sci. Robot.*, vol. 1, no. 1, 2016, Art. no. eaai7529.

[26] Y. Mori *et al.*, "Development of a pneumatically driven flexible finger with feedback control of a polyurethane bend sensor," in *Proc. IEEE/RSJ Int. Conf. Intell. Robots Syst.*, 2018, pp. 5952–5957.

[27] G. Soter, M. Garrad, A. T. Conn, H. Hauser, and J. Rossiter, "Skinflow: A soft robotic skin based on fluidic transmission," in *Proc. IEEE Int. Conf. Soft Robot.*, 2019, pp. 355–360.

[28] M. D. Dickey, R. C. Chiechi, R. J. Larsen, E. A. Weiss, and D. A. Weitz, "Eutectic gallium-indium (EGaIn): A liquid metal alloy for the formation of stable structures in microchannels at room temperature," *Adv. Functional. Mater.*, vol. 18, no. 7, pp. 1097–1104, 2008.

[29] Texas Instruments, Dallas, TX, USA. Inductance-to-digital converter chip LDC1614, 2019. [Online]. Available: http://www.ti.com/product/LDC1614/

[30] K. C. Galloway, P. Polygerinos, C. J. Walsh, and R. J. Wood, "Mechanically programmable bend radius for fiber-reinforced soft actuators," in *Proc. 16th Int. Conf. Adv. Robot.*, 2013, pp. 1–6.